

Spring 5-3-2011

Gas-Solids Hydrodynamics in a CFB with 6 Cyclones and a Pang Leg

Lemigh Cheng

State Key Laboratory of Clean Energy Utilization, Zhejiang University, Hangzhou

Xinglong Zhou

State Key Laboratory of Clean Energy Utilization, Zhejiang University, Hangzhou

Chao Wang

State Key Laboratory of Clean Energy Utilization, Zhejiang University, Hangzhou

Qinhui Wang

State Key Laboratory of Clean Energy Utilization, Zhejiang University, Hangzhou

Zhongyang Luo

State Key Laboratory of Clean Energy Utilization, Zhejiang University, Hangzhou

See next page for additional authors

Follow this and additional works at: <http://dc.engconfintl.org/cfb10>

 Part of the [Chemical Engineering Commons](#)

Recommended Citation

Lemigh Cheng, Xinglong Zhou, Chao Wang, Qinhui Wang, Zhongyang Luo, Kefa Cen, Li Nie, Chaogang Wu, and Qi Zhou, "Gas-Solids Hydrodynamics in a CFB with 6 Cyclones and a Pang Leg" in "10th International Conference on Circulating Fluidized Beds and Fluidization Technology - CFB-10", T. Knowlton, PSRI Eds, ECI Symposium Series, (2013). <http://dc.engconfintl.org/cfb10/55>

This Conference Proceeding is brought to you for free and open access by the Refereed Proceedings at ECI Digital Archives. It has been accepted for inclusion in 10th International Conference on Circulating Fluidized Beds and Fluidization Technology - CFB-10 by an authorized administrator of ECI Digital Archives. For more information, please contact franco@bepress.com.

Authors

Lemigh Cheng, Xinglong Zhou, Chao Wang, Qinhui Wang, Zhongyang Luo, Kefa Cen, Li Nie, Chaogang Wu,
and Qi Zhou

GAS-SOLIDS HYDRODYNAMICS IN A CFB WITH 6 CYCLONES AND A PANT LEG

Leming Cheng ^a, Xinglong Zhou ^a, Chao Wang ^a, Qinhui Wang ^a, Zhongyang Luo^a,
Kefa Cen ^a, Li Nie ^b Chaogang Wu ^b, Qi Zhou ^b

^a State Key Laboratory of Clean Energy Utilization, Zhejiang University, Hangzhou
310027, China

^b Dongfang Boiler Group Co., Ltd. Chengdu 611731, China

ABSTRACT

Solids volume fraction and particle velocity profiles were measured with a fiber optical probe in a cold circulating fluidized bed test rig with 6 parallel cyclones and a pant leg. Results in the pant leg zone, main bed zone and exit zone of the furnace are reported. The work also includes the influences of superficial gas velocity, secondary air rate and static bed height on the gas-solids hydrodynamics.

INTRODUCTION

Circulating fluidized beds (CFBs) are commercially employed in a number of gas–solids contacting processes such as fluid catalytic cracking, fossil fuel combustion and gasification (1). Knowledge of the gas-solids hydrodynamics is the key to understanding and predicting chemical interactions between gas and particles, heat transfer performance and erosion in the furnace (2).

The majority of previous experimental studies of solid flux profiles have been carried out in CFBs with single furnaces (3-5). In single furnace, a typical core-annulus flow pattern has been observed by many researchers in laboratory and industrial scale units (5-7). However, the structure of a CFB furnace is becoming more and more complex during scale-up, especially in recent development of a 600MW CFB boiler. Large-scale CFB furnaces have new characteristics, i.e. multiple outlets, pant legs and internal walls. Few studies have been conducted and reported on lateral solids flow in the riser with a pant leg structure. Therefore, further study on the gas-solids hydrodynamics in a large-scale CFB furnace is required to provide more understanding of the flow structure.

In this study, solids volume fraction and particle velocity profiles in a CFB with 6 cyclones and a pant leg furnace were investigated by using a fiber optical probe (FOP). The work focused on three zones in the furnace, the lower pant leg zone, the main bed zone and the exit zone of the furnace. Effects of superficial gas velocity, secondary air rate and static bed height on the solids volume fraction and particle

velocity distributions were examined. This was a part of the work conducted to develop the 600MW CFB boiler.

EXPERIMENTAL

The experiments were done in the CFB cold model system shown in Fig. 1. The test rig was scaled down from a 600 MW CFB boiler (8) following the scaling law proposed by Glicksman et al (9). The riser had a height of 5.5 m and the bottom section of the riser looks like a pair of pants (pant leg structure). The internal walls of the pant leg were 1 m high. Above 1 m from the gas distributors, the riser had a cross-sectional area of $0.422 \times 0.727 \text{ m}^2$. 6 parallel cyclones were located asymmetrically on the left and right walls of the riser (Fig. 2). Circulating loops were formed with the pant leg riser, 6 cyclones, 6 standpipes and 6 loopseals. Most of the apparatus was made of Plexiglas for convenient observation. The measurements were conducted at atmospheric pressure and ambient temperature.

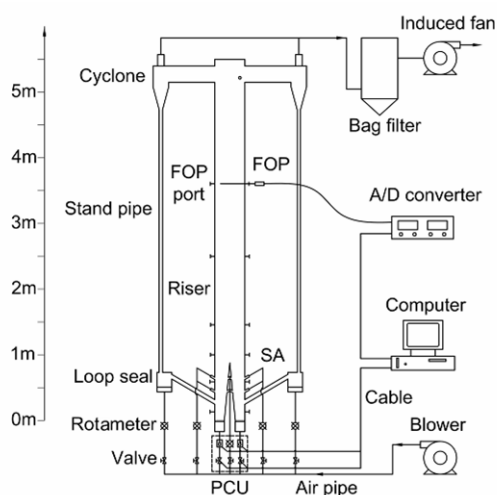


Fig. 1. Experimental CFB cold test rig

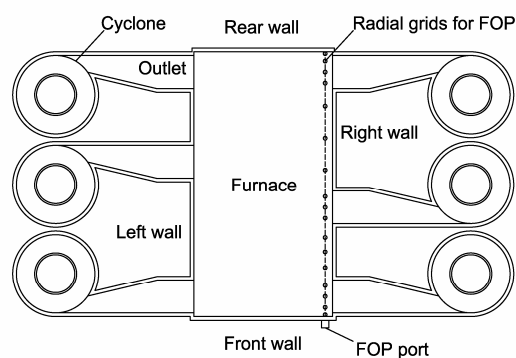


Fig. 2. Layout of the 6 parallel cyclones

During operation, the solids fluidization in the individual pant legs was controlled by independent primary air flow. Bed pressures in the two pant legs were kept in balance by a pressure control unit (PCU).

The Fiber optical probe (FOP) method (10-12) was used to measure the solids volume fraction and the particle velocity in the riser. The probe measurement system (PV6D) was composed of an optical fiber probe, a control system, an A/D converter and a data acquisition system. It was calibrated before the measurements were made (13).

The FOP measurements were taken at seven different height levels (level 1: 0.25, level 2: 0.65, level 3: 1, level 4: 1.45, level 5: 2.55, level 6:3.65 and level 7: 5.25 m) above the air distributors as shown in Fig. 1. At locations from level 1 to level 6, the fiber optic probe was traversed from the left wall to the right wall. It was traversed from the front wall to the rear wall at level 7, as shown in Fig. 2. It should be noted that a positive value for the particle velocity means the particle moves upward in the riser at levels 1 ~ 6 and flows toward the cyclones at level 7.

Glass beads with a density of 2364 kg/m³ and an average particle diameter of 0.114 mm were used as bed materials. The effects of superficial gas velocity (u_0), secondary air rate (R_{SA}) and static bed height (H_s) on the solids volume fraction and particle velocity profiles were studied in the experiments. The bed material properties and the operational parameters of the boiler and model are shown in Table 1.

Table 1. Bed material properties and operational parameters

Parameter	Unit	Boiler	Model
Temperature, T_b	°C	900	50
Gas density, ρ_g	kg/m ³	0.301	1.093
Gas viscosity, V_s	m ² /s	1.55E-04	1.80E-05
Mean particle diameter of, d_p	mm	0.400	0.114
Density of particle, ρ_s	kg/m ³	2000	2364
Superficial gas velocity, u_0	m/s	-	1.7
Minimum fluidization velocity, u_{mf}	m/s	0.050	0.016
Solid flux, G_s	kg/m ² s	-	6.00

RESULTS AND DISCUSSION

Solids volume fraction and particle velocity profiles in the pant leg, main bed and exit zone

Fig. 3 shows the solids volume fraction (ϵ_s) and particle velocity (u_p) profiles at level 2 (within the pant leg section, 0.65 m above the gas distributors) for $u_0 = 1.7$ m/s, $R_{SA} = 10$ % and $H_s = 500$ mm. Corresponding results for the left and right pant leg show similar distributions of ϵ_s and u_p although the particles in the two pant leg furnaces are fluidized independently. The solids volume fraction increased near the walls since it requires less energy for the bubbles to pass through the center of the bed (14). Particle velocity decreased near the walls, and a negative axial solids velocity appeared near the wall.

Lateral profiles of ϵ_s and u_p at level 3 (top- section of the pant leg, 1 m above the gas distributors) at the same conditions of Fig. 3 are shown in Fig. 4. A W-shaped

distribution of the solids volume fraction and an M-shaped distribution of the particle velocity are seen in Fig. 4. Solid boundary layers exist near the side walls and the internal walls of the pant leg. The solids volume fraction in the boundary layer is higher than in the core zone. The maximum solids volume fraction in the boundary layer near the internal walls was even higher than in the boundary layer near the side walls. It was found that the downflow of particles in the boundary layers had different downflow velocities at different locations. The downflow particles near the enclosure walls had higher velocities (1.5 ~ 2 m/s) than that near the pant leg internal walls (below 1 m/s).

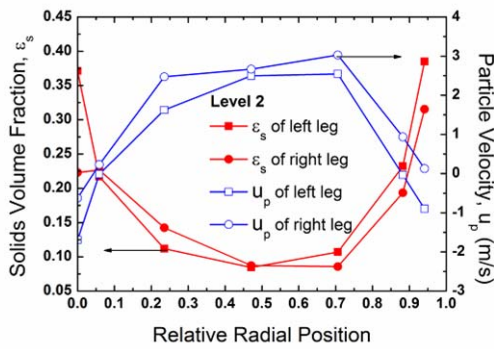


Fig. 3. Profiles of ϵ_s and u_p at level 2

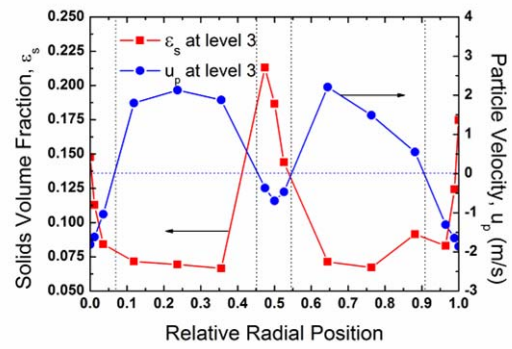


Fig. 4. Profiles of ϵ_s and u_p at level 3

The above results on ϵ_s and u_p profiles in Fig. 3 and Fig. 4 give a general picture of the gas-solids flow pattern in the pant leg zone. Within the pant leg zone, two core-annulus flow structures are formed independently. These two cores are merged into one core at the top of the pant legs and then a W-shaped profile of solids volume fraction and an M-shaped profile of particle velocity are formed.

Above the pant leg section, the riser is a single furnace. Fig. 5 shows ϵ_s and u_p profiles at level 4 (1.45 m above the air distributors) and shows a transitional flow pattern from the two core-annulus structures to a traditional core-annulus structure. The particle velocity profile has completely transitioned, but the solids volume fraction profile still is higher in the center of the furnace.

Fig. 6 shows ϵ_s and u_p profiles of a traditional core-annulus flow structure in the upper dilute section of the riser (at level 5, 2.55 m above the air distributors). The boundary layer thickness is defined as the distance from the wall to the position of zero particle velocity, i.e. the position separating the particle upflow in the bed core and the particle downflow near the wall (7). From the areas marked out by the dotted lines in Figs 4 to 6, the boundary layer thickness is about 5 to 15 mm which decreases slightly with the height of the riser. This is in agreement with results from literature (6).

Inside the core zone, the ϵ_s and u_p profiles are both flat with an average ϵ_s of approximately 0.017 and an average u_p of about 1 m/s. The particles in the boundary layer have a downflow velocity which varies from 0.7 to 1.5 m/s depending on location. The downflow velocity reaches a lower value of about 0.7 m/s near the wall. This suggests a momentum transfer between the falling film and the wall, which is likely to depend on the properties of the wall surface (surface roughness of wall, inclination of surfaces from the vertical direction, etc.). The resulting solids volume fraction and particle velocity distributions are similar to measurements reported by Zhang et al. (Z) .

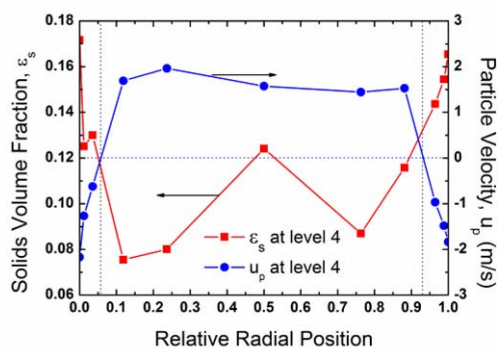


Fig. 5. Profiles of ϵ_s and u_p at level 4

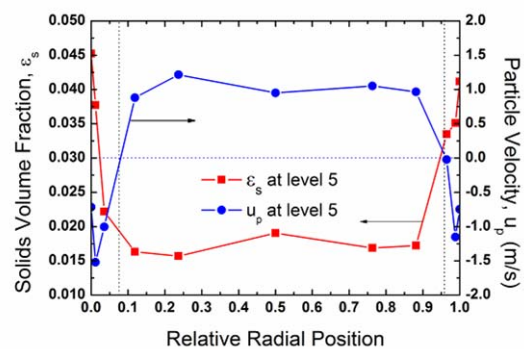


Fig. 6. Profiles of ϵ_s and u_p at level 5

The ϵ_s and u_p distributions at the exit section presented in Fig. 7 were measured at level 7 (near the horizontal ducts, 5.25 m above the air distributors). Due to the complicated structure of the exit section and the asymmetric layout of the cyclones, solids volume fraction and particle velocity were not evenly distributed across the furnace. Of the three outlets indicated by the dotted lines in Fig. 7, a slightly higher particle velocity and a lower solids volume fraction were measured for the middle outlet (outlet B).

Effect of superficial gas velocity, secondary air rate and static bed height

The evolution of the ϵ_s and u_p profiles as a function of superficial gas velocity (u_0) is shown in Fig. 8. The results were measured at level 5 for a secondary air rate of 10 % and a static bed height of 500 mm. The solids volume fraction in the core zone increased with increasing superficial gas velocity. When u_0 increases more particles are entrained into the upper section of the riser. However, the superficial gas velocity did not show a significant impact on solids volume fraction in the boundary layer. Moreover, in spite of increasing superficial gas velocity, it did not have a significant effect on particle velocity.

Fig. 9 shows ϵ_s and u_p profiles at a constant superficial gas velocity ($u_0 = 1.70$ m/s) and static bed height ($H_s = 500$ mm) but at different secondary air rates (R_{SA}). It can be seen that at level 6, the solids volume fractions in both the core zone and the boundary layer decrease when secondary air rate increases from 10 % to 20 %. The difference in the solids volume fraction is most likely, because of the barrier effect of the secondary air (15). The particle velocity in the core decreases when R_{SA} increases due to the reduction in the acceleration of the particles due to primary air (16).

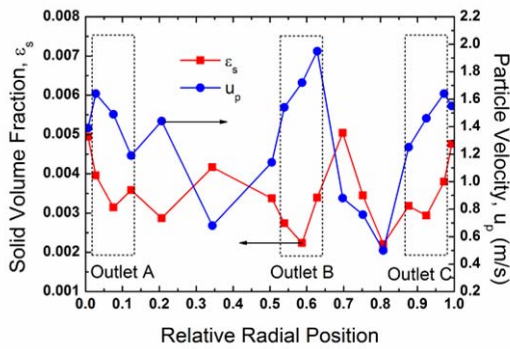


Fig. 7. Profiles of ϵ_s and u_p at level 7

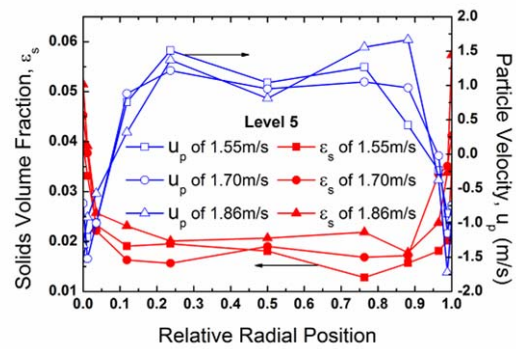


Fig. 8. Profiles of ϵ_s and u_p for different u_0

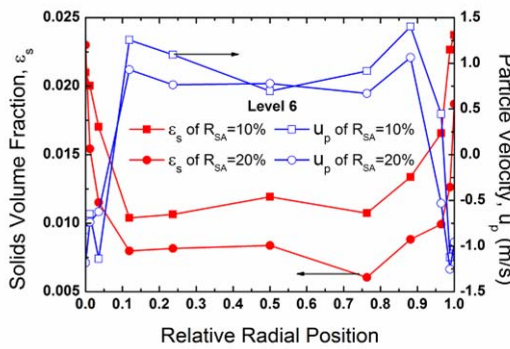


Fig. 9. Profiles of ϵ_s and u_p for different R_{sa} at level 6

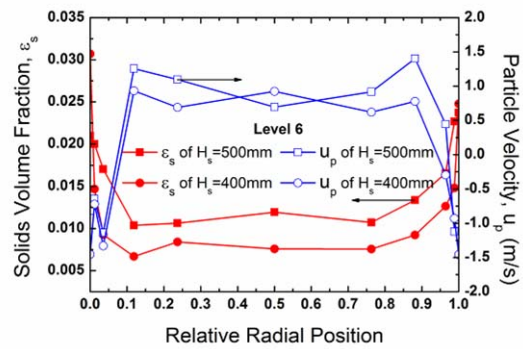


Fig. 10. Profiles of ϵ_s and u_p for different H_s at level 6

Fig. 10 shows ϵ_s and u_p profiles at level 6 in the furnace for different static bed heights ($H_s = 400$ and 500 mm). The solid volume fractions in both the core zone and the boundary layer when $H_s = 500$ mm were higher than that for a lower H_s . This is reasonable because a higher H_s results in a higher average solids volume fraction in the whole furnace. Comparing the u_p profiles in Fig. 10, it can be seen that u_p in the core zone increases slightly with H_s while no clear influence is observed in the boundary layer.

CONCLUSIONS

The results of the investigation show that within the pant leg section, two core-annulus flow structures are formed independently. These two cores are merged into one core above the pant leg section and the solids flow pattern makes a transition to a traditional core-annulus structure. The boundary layer thickness is about 5 to 20 mm which decreases slightly with riser height. The particles in the boundary layer have a downflow velocity which varies from 0.7 to 1.5 m/s. Due to the asymmetric layout of the three riser outlets on each side wall, a higher particle velocity and a lower solids volume fraction were observed in the middle outlet.

The solids volume fraction in the upper section of the riser increases with superficial gas velocity and static bed height but decreases with secondary air rate. Particle velocity in the core zone of the upper riser section increases with static bed height and decreases with secondary air rate. There was no significant influence of bed height on particle velocity in the boundary layer.

ACKNOWLEDGEMENT

The authors are grateful for financial support of the National Key Technologies R & D Program of China (No. 2006BAA03B02-08, 2006BAA03B01-09).

NOTATION

d_p : Mean diameter of particle [mm]	u_0 : Superficial gas velocity [m/s]
G_s : Solid flux [$\text{kg}/\text{m}^2\text{s}$]	u_{mf} : Minimum fluidization velocity [m/s]
H : Height of the riser [m]	u_p : Particle velocity [m/s]
H_s : Static bed height [mm]	ν_s : Gas viscosity [m^2/s]
D : Depth of the riser's cross-section [m]	ϵ_s : Solids volume fraction [-]
X : Radial position from left wall [m]	ρ_s : Solids density [kg/m^3]
R_{SA} : Secondary air rate [%]	ρ_g : Gas density [kg/m^3]
T_b : Bed temperature [$^{\circ}\text{C}$]	

REFERENCES

1. Cheng LM, Chen B, Liu N, Luo ZY, Cen KF. Effect of characteristic of sorbents on their sulfur capture capability at a fluidized bed condition. *Fuel* 2004; 83: 925-932.
2. Basu P. Combustion of coal in circulating fluidized-bed boilers: a review. *Chemical Engineering Science* 1999; 54: 5547-5557.
3. Ye S, Qi XB, Zhu J. Direct Measurements of Instantaneous Solid Flux in a

Circulating Fluidized Bed Riser using a Novel Multifunctional Optical Fiber Probe. *Chem Eng Technol* 2009; 32: 580-589.

4. Malcus S, Cruz E, Rowe C, Pugsley TS. Radial solid mass flux profiles in a high-suspension density circulating fluidized bed. *Powder Technology* 2002; 125: 5-9.
5. Salvaterra A, Geldart D, Ocone R. Solid flux in a circulating fluidized bed riser. *Chem Eng Res Des* 2005; 83: 24-29.
6. Kim SW, Kirbas G, Bi HT, Lim CJ, Grace JR. Flow structure and thickness of annular downflow layer in a circulating fluidized bed riser. *Powder Technology* 2004; 142: 48-58.
7. Zhang WN, Johnsson F, Leckner B. Fluid-Dynamic Boundary-Layers in CFB Boilers. *Chemical Engineering Science* 1995; 50: 201-210.
8. Li Y, Nie L, Hu XK, Yue GX, Li WK, Wu YX, Lu JF, Che DF. Structure and performance of a 600MWe supercritical CFB boiler with water cooled panels. In: 20th International Conference on Fluidized Bed Combustion. Xian, China, 2009: 132-136.
9. Glicksman LR, Hyre M, Woloshun K. Simplified Scaling Relationships for Fluidized-Beds. *Powder Technology* 1993; 77: 177-199.
10. Li SH, Yang HR, Zhang H, Yang S, Lu JF, Yue GX. Measurements of solid concentration and particle velocity distributions near the wall of a cyclone. *Chem Eng J* 2009; 150: 168-173.
11. Werther J. Measurement techniques in fluidized beds. *Powder Technology* 1999; 102: 15-36.
12. Zhu JX, Li GZ, Qin SZ, Li FY, Zhang H, Yang YL. Direct measurements of particle velocities in gas-solids suspension flow using a novel five-fiber optical probe. *Powder Technology* 2001; 115: 184-192.
13. Zhang H, Johnston PM, Zhu JX, de Lasa HI, Bergougnou MA. A novel calibration procedure for a fiber optic solids concentration probe. *Powder Technology* 1998; 100: 260-272.
14. Guo QJ, Werther J. Flow behaviors in a circulating fluidized bed with various bubble cap distributors. *Ind Eng Chem Res* 2004; 43: 1756-1764.
15. Koksai M, Hamdullahpur F. Gas mixing in circulating fluidized beds with secondary air injection. *Chem Eng Res Des* 2004; 82: 979-992.
16. Ersoy LE, Golriz MR, Koksai M, Hamdullahpur F. Circulating fluidized bed hydrodynamics with air staging: an experimental study. *Powder Technology* 2004; 145: 25-33.